

## Dose Rate Determination of Gamma Rays Emitted by Thallium-201 and Technetium-99m Using a Modified Horseradish Peroxidase Based Biosensing System

M. Shourian<sup>a</sup>, H. Ghourchian<sup>a,\*</sup>, H.-A. Rafiee-Pour<sup>a</sup> and H. Tavakoli<sup>b</sup>

<sup>a</sup>Laboratory of Microanalysis, Institute of Biochemistry and Biophysics, University of Tehran, P.O. Box 13145-1384, Tehran, Iran

<sup>b</sup>Faculty of Medicine, Department of Physiology and Biophysics, Baghiyatollah University of Medical Sciences, Tehran, Iran

(Received 4 December 2009, Accepted 5 February 2010)

In the presence of low energy gamma emitter radioisotopes of thallium-201 (<sup>201</sup>Tl) or technetium-99m (<sup>99m</sup>Tc), H<sub>2</sub>O<sub>2</sub> was generated *via* radiolysis of water. The produced H<sub>2</sub>O<sub>2</sub> was amperometrically determined using an anthraquinone 2-carboxylic acid modified horseradish peroxidase on glassy carbon electrode. In the presence of each radioisotope, the cathodic current produced due to the amperometric detection of H<sub>2</sub>O<sub>2</sub>, was designated as biosensor response. At the applied potential of -550 mV (*vs.* Ag/AgCl), the biosensor showed the sensitivities of 1.937 and 2.278 nA h μGy<sup>-1</sup> towards H<sub>2</sub>O<sub>2</sub> produced by <sup>201</sup>Tl and <sup>99m</sup>Tc respectively. Finally, the calibration curves for dose rate determination of <sup>201</sup>Tl and <sup>99m</sup>Tc have been presented and the correlations between biosensor response to H<sub>2</sub>O<sub>2</sub> and the gamma emitter dose rates for <sup>201</sup>Tl and <sup>99m</sup>Tc are established.

**Keywords:** Thallium-201, Technetium-99m, Gamma ray, Hydrogen peroxide, Horseradish peroxidase, Anthraquinone 2-carboxylic acid

---

### INTRODUCTION

Gamma rays are highly energetic electromagnetic, uncharged, and indirectly ionizing radiations which are emitted during a nuclear reaction. Basically, these rays interact with matter *via* two main processes of ionization and excitation [1]. When gamma rays interact with molecules, the stored energy brings about molecule ionization. Since the water content of living cells is approximately 70%, the majority of ionization produced by gamma rays, take place through water molecules interactions. This process is called water radiolysis [2,3]. Radiolysis of cellular water will produce reactive oxygen derivatives such as the hydroxyl radical (OH<sup>•</sup>) that may interact with cellular component and

macromolecules (DNA and proteins). In the absence of cell repair mechanism, such interaction afflicts sub-cellular structure and leads to the cell death [4,5]. To date, conventional monitors such as Geiger-Muller ionization chamber, proportional counters and gas-flow counters, as three different types of gas-filled detectors, and also scintillation and semiconductor detectors have been utilized for the determination of gamma rays.

Various types of reactive oxygen species could be produced by radiolysis of water. The free radicals of superoxide (O<sub>2</sub><sup>•-</sup>) and OH<sup>•</sup> are two major products of water irradiation. There is a possibility of hydrogen peroxide (H<sub>2</sub>O<sub>2</sub>) production by combining OH<sup>•</sup> radicals. H<sub>2</sub>O<sub>2</sub> as an oxidizing agent is able to damage cells, tissues and various organs. Therefore, determination of H<sub>2</sub>O<sub>2</sub> is of significance in radiobiology and medical investigations [6].

---

\*Corresponding author. E-mail: hadi@ibb.ut.ac.ir

The conventional techniques developed for the determination of  $H_2O_2$  are spectrophotometry [7], fluorimetry [8], electrochemical methods [9], chemiluminescence [10], electron spin resonance (ESR) [11] and colorimetry [12]. Some of these techniques such as spectrophotometry, fluorimetry and colorimetry can determine  $H_2O_2$  in water media qualitatively. Some others, such as ESR need complicated and expensive equipment as well as necessary professional expertise. Among these techniques, electrochemical method has the desirable characteristics such as high sensitivity and selectivity, low cost, and simple instrumentation.

In the present research, the  $H_2O_2$  produced by two gamma emitter radioisotopes of thallium-201 ( $^{201}Tl$ ) and technetium-99m ( $^{99m}Tc$ ) was detected by a novel electrochemical method.  $^{201}Tl$  and  $^{99m}Tc$  are two favorite gamma emitter radioisotopes in nuclear medicine which are widely used as approved radio-imaging drugs and in nuclear medicine imaging procedures. These radioisotopes are ideal for both external radiation detection and the patient's exposure to low radiation. The  $H_2O_2$  produced by these gamma emitters was detected by anthraquinone 2-carboxylic acid (AQ) modified horseradish peroxidase (HRP) as a specific bio-sensing system. In addition, the dose rates for  $^{201}Tl$  and  $^{99m}Tc$  were determined by establishing a correlation between the generated  $H_2O_2$  and the applied doses of gamma emitters.

## EXPERIMENTAL

### Reagents and Radioisotopes

HRP (EC 1.11.1.7), sodium 4-(2-hydroxyethyl)-1-piperazine ethansulfonate (Na-HEPES), AQ 98%,  $H_2O_2$  30% (w/w) solution, 4-aminoantipyrine 98% (4-AAP), 1-(3-dimethylaminopropyl)-3-ethyl carbodiimide hydrochloride 98% (DEC) were purchased from Sigma, St. Louis, MO. Superfine Sephadex G-25 was obtained from Pharmacia LKB, Uppsala, Sweden.

$^{201}Tl$  (gamma ray energy of 70-80 Kilo Electron Volt; KeV, half-life of 72.912 hours) and  $^{99m}Tc$  (elution from molybdenum-technetium generator in the chemical form of pertechnetate anion,  $TcO_4^-$ , half life 6 hours and gamma ray energy of 140 KeV) were purchased from Atomic Energy Organization of Iran. To measure the dose rates, the absorbed radiation doses were controlled by injection of different

volumes of  $^{201}Tl$  or  $^{99m}Tc$  into single-compartment cell equipped with a platinum auxiliary electrode, an Ag/AgCl reference electrode containing 3 M KCl, (Metrohm) and fabricated biosensor as working electrode. Before each test, the equivalent absorbed dose rates were directly determined by a Geiger-Muller dosimeter (Rados Dosimeter).

### Modification of HRP

The modification of HRP with AQ was made according to our previously reported procedure [13,14]. Briefly, AQ (5 mg) was suspended in 3 ml of Na-HEPES solution (0.15 M, pH 7.2). Then, 6.5 mg of DEC was dissolved in solution. The enzyme was added to the Na-HEPES-DEC solution and the mixture was stirred for 20 h by magnetic stirrer at 4 °C. The turbid solution was centrifuged for 4 min and the supernatant was further purified *via* gel filtration. Finally, the concentration of the AQ-modified HRP (AQ-HRP) was determined using the Bradford method [15].

### Specific Biosensing System

The specific bio-sensing system was prepared as follows. At first, the surface of glassy carbon electrode was mechanically polished twice by 10 and 0.3 micron alumina powder, respectively. Then, it was washed by double-distilled de-ionized water. The polished electrode was placed in a 0.2 M potassium phosphate buffer (pH 7.0) while, to activate the electrode surface, an anodic potential of 1.70 V was applied for 1 min. Finally, the GC electrode was immersed in the solution of 0.4 mg ml<sup>-1</sup> of AQ-HRP in 0.2 M potassium phosphate buffer (pH 7.0) for 1 h. Finally, in the same solution, the electrode was treated between -300 and -700 mV (*vs.* Ag/AgCl) at a sweep rate of 100 mV s<sup>-1</sup> for approximately 100 cycles. This process brought about a stable current response in both cyclic voltammetry and amperometry.

### Hydrogen Peroxide Detection

Detection of  $H_2O_2$  was carried out using both cyclic voltammetry and amperometry. For this purpose, the electrode prepared according to the above-mentioned procedure was dipped in the solution of 0.4 mg ml<sup>-1</sup> of AQ-HRP in 0.2 M potassium phosphate buffer (pH 7.0), and the cyclic voltammograms (CVs) or amperograms were obtained in the absence or presence of  $H_2O_2$ . In order to determine the  $H_2O_2$  produced by gamma rays emitted from  $^{201}Tl$  or  $^{99m}Tc$ , different

dose rates of  $^{201}\text{Tl}$  or  $^{99\text{m}}\text{Tc}$  were added to the test solution and  $\text{H}_2\text{O}_2$  was detected using the mentioned procedure. All CVs were obtained at the potential scan rate of  $20 \text{ mV s}^{-1}$ . Before the measurements, the experimental solutions were de-aerated by highly pure nitrogen for 10 min and a nitrogen atmosphere was kept over the solutions during the measurements. The amperograms were obtained at the constant potential of  $-550 \text{ mV vs. Ag/AgCl}$ .

All CVs and amperograms, both in the presence and absence of gamma emitter radioisotopes ( $^{201}\text{Tl}$  or  $^{99\text{m}}\text{Tc}$ ), were recorded by using a Potentiostat/Galvanostat (model 263-A, EG&G, USA) equipped with "Power Suite" software package and a rotating disk electrode (model 616, PerkinElmer, USA). All measurements were carried out at room temperature.

## RESULT AND DISCUSSION

### AQ-HRP Behavior at Interface

To analyze the interaction between the AQ-HRP molecules

in the solution with the electrode surface molecules, the *in situ* behavior of AQ-HRP on GC electrode was recorded by cyclic voltammetry. Figure 1A shows some selected cycles out of 100 CVs. From inset 1-A, it is clear that the process for enzyme adsorption on GC electrode was in progress by increasing the number of cycles until it finally reaches a plateau around 90 cycles. Such a behavior could be due to adsorption, growth and formation of AQ-HRP film on the electrode surface. Similar results have been reported for the adsorption of some quinone derivatives of electrochemically activated glassy carbon electrodes [16]. This behavior is referred to as the properties of the attached AQ to accessible lysine groups on HRP surface. Since the AQ ring structure and GC electrode surface are both hydrophobic, this leads to the hydrophobic-hydrophobic interaction between them in aqueous media.

However, applying an anodic potential of  $1.70 \text{ V (vs. Ag/AgCl)}$  to the GC electrode builds up the hydrophilic functional groups on the electrode surface. This prepares the

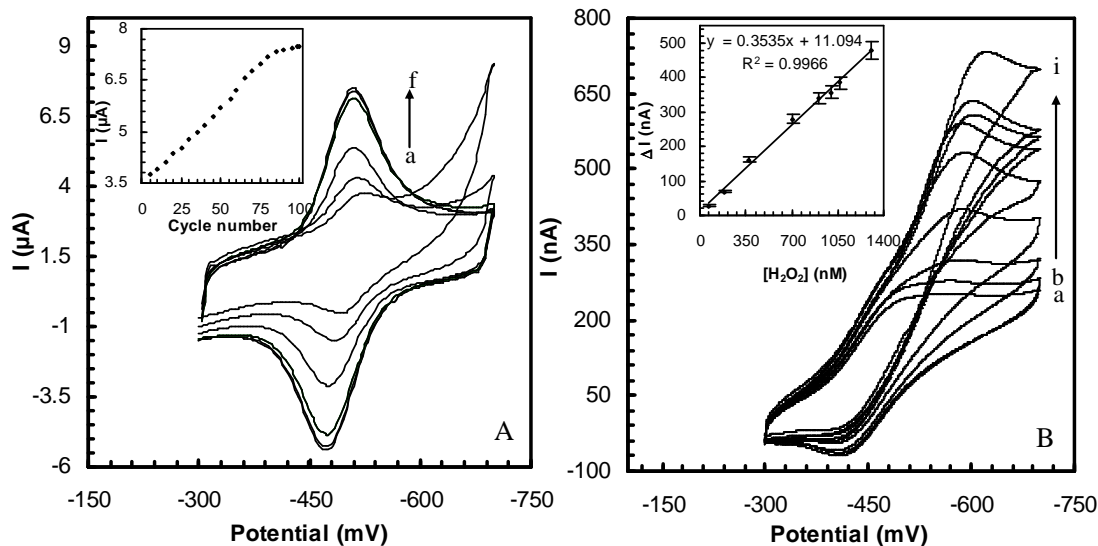


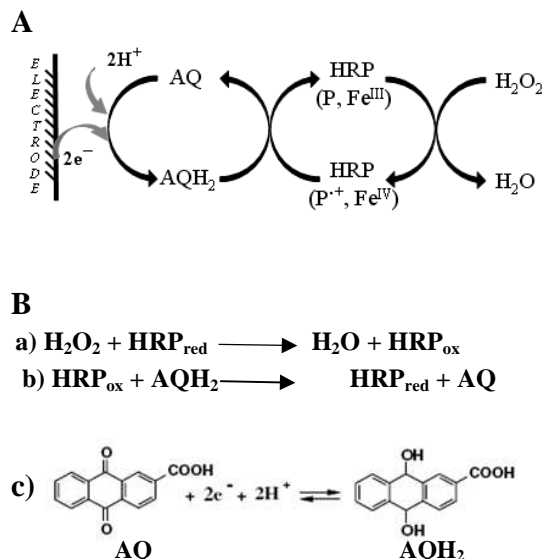
**Fig. 1.** (A) *In situ* adsorption of HRP-AQ on GC electrode. Curves a-f, represent the CVs of HRP-AQ on GC electrode at cycle number 3, 19, 50, 60, 90 and 100, respectively. Inset shows the  $I_{pc}$  obtained by the CVs of HRP-AQ vs. the cycle number of CVs. The scan rate was  $100 \text{ mV s}^{-1}$ . (B) CVs of HRP-AQ on GC electrode in the presence of  $\text{H}_2\text{O}_2$ . Curves a-i, were obtained in the presence of 0, 70, 188, 376, 712, 905, 1005, 1075 and 1307 nM of  $\text{H}_2\text{O}_2$ , respectively. The inset represents the  $\Delta I_{pc}$  against  $\text{H}_2\text{O}_2$  concentration.  $\Delta I_{pc}$  is the difference between the cathodic peak current obtained in the presence of certain concentration of  $\text{H}_2\text{O}_2$  (CVs b to i) and that in the absence of  $\text{H}_2\text{O}_2$  (CV a). The scan rate was  $20 \text{ mV s}^{-1}$ . For details see text.

surface for electrostatic and dipole interactions with the modified enzyme. In our previous study, it was shown that only a monolayer of modified enzyme is formed on GC electrode which is able to detect  $\text{H}_2\text{O}_2$  within the linear range of  $2.65 \times 10^{-9}$  to  $1.08 \times 10^{-7}$  M [17]. Further studies showed that at higher concentrations of  $\text{H}_2\text{O}_2$  the AQ-HRP molecules, both in the adsorbed layer and in the solution, could contribute to current responses.

### Electrochemistry of AQ-HRP Solution on GC Electrode

Chemical modification of HRP by AQ, followed by adsorption of the HRP-AQ on glassy carbon (GC) electrode, established a fast and efficient electron transfer between the electrode surface and the redox center of peroxidase. This modification not only makes the HRP more conductive, but it also enhances the catalytic activity of the enzyme and lowers the enzyme redox potential as well [13,14]. The lowering of the enzyme may minimize the interference of some electro-oxidizable biological fluid constituents [18,19]. Although the behavior of this method can be explained from Scheme I, the true mechanism for electron transferring is far more complicated. Scheme 1A demonstrates the electron transfer process on the surface of GC electrode. The determination of  $\text{H}_2\text{O}_2$  could be explained based on the successive reactions from a to c (Scheme 1B). The added  $\text{H}_2\text{O}_2$  in the buffered solution is reduced by the modified HRP (reaction a) while the heme prosthetic group is oxidized. To recover the enzyme, the reduced form of mediator ( $\text{AQH}_2$ ) is oxidized to its oxidized form (AQ) (reaction b). Finally, in the applied potential of -479 mV, AQ is reduced to  $\text{AQH}_2$  at the electrode surface (reaction c). The cathodic current generated by this step of the redox reaction is directly proportional to the  $\text{H}_2\text{O}_2$  concentration.

To observe the electrochemical behavior of AQ-HRP solution on GC electrode, cyclic voltammetric experiments were carried out in the presence of different concentrations of  $\text{H}_2\text{O}_2$ . As shown in Fig. 1B, upon the addition of  $\text{H}_2\text{O}_2$  in the concentration range of 70 nM to 1.31  $\mu\text{M}$  into the buffered solution, a significant current response was observed. Furthermore, as seen in Fig. 1B, the  $I_{pc}$  shifted toward more negative values with increasing  $\text{H}_2\text{O}_2$ . It seems that in addition to the adsorbed AQ-HRP, the dissolved AQ-HRP molecules



Scheme 1. (A) Representation of electron transfer between HRP and GC electrode based on shuttling role of AQ molecules, (B) the bio-electrocatalytic and electrochemical reactions at biosensor interface. AQ and  $\text{AQH}_2$  show the oxidized and reduced forms of anthraquinone 2-carboxylic acid, respectively.

are also accessible to the electrode. Upon increasing the  $\text{H}_2\text{O}_2$  concentration, the current significantly increases. Consequently, the dissolved AQ-HRP molecules start to contribute to the produced current. Thus, their mass transport could establish a concentration overpotential resulting in the observed  $I_{pc}$  shift in Fig. 1B. The 1B-inset shows the extent of increments in the cathodic peak current ( $\Delta I_{pc}$ ) upon increasing the  $\text{H}_2\text{O}_2$  concentration. As shown, the increasing of cathodic current is directly proportional to the concentration of  $\text{H}_2\text{O}_2$  in the bulk solution.  $\Delta I_{pc}$  appears to display first-order behavior, changing linearly with  $\text{H}_2\text{O}_2$  concentration range from 70 to 1307 nM with the sensitivity of  $0.35 \text{ nA nM}^{-1}$  and detection limit of 7.15 nM at a signal to noise ratio of 3 (s.d. 0.834).

### Cyclic Voltammetry of AQ-HRP in the Presence of $^{201}\text{Tl}$ or $^{99m}\text{Tc}$

Figure 2 illustrates cyclic voltammetric responses of the biosensor toward  $\text{H}_2\text{O}_2$  produced by  $^{201}\text{Tl}$  and  $^{99m}\text{Tc}$ ,

## Dose Rate Determination of Gamma Rays Emitted by Thallium-201

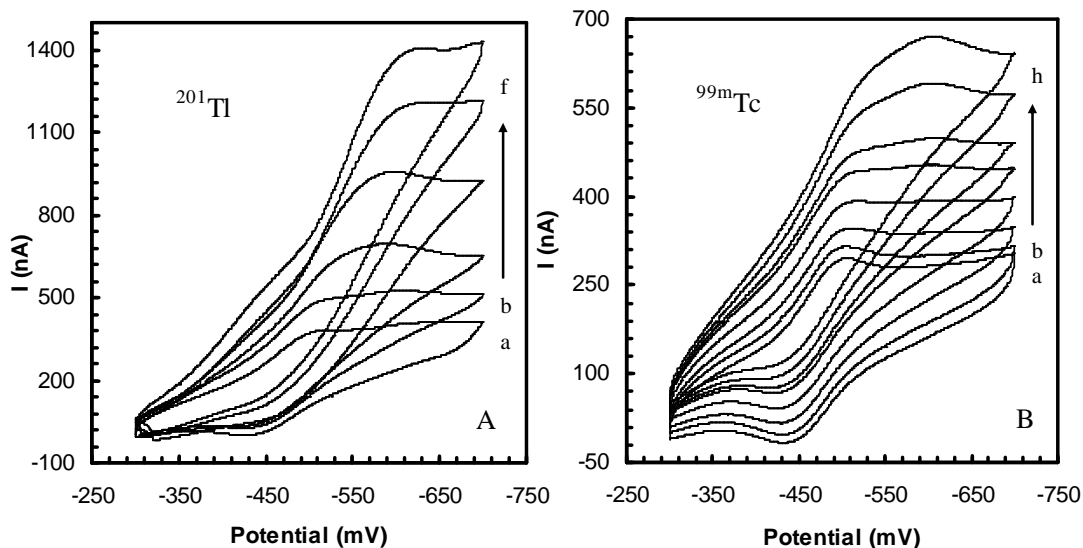


**Fig. 2.** (A) CVs of HRP-AQ on GC electrode in the presence of  $^{201}\text{Tl}$ . Curve a was obtained by dipping the HRP-AQ on GC electrode in PBS. The CVs from b to h are the same as a, but in the presence of different  $^{201}\text{Tl}$  dose rates of 135, 312, 759, 934 and  $1102 \mu\text{Gy h}^{-1}$ , respectively. (B) CVs of HRP-AQ on GC electrode in the presence of  $^{99\text{m}}\text{Tc}$ . Curve a was obtained by dipping the HRP-AQ on GC electrode in PBS. The CVs from b to h are the same as a, but in the presence of different  $^{99\text{m}}\text{Tc}$  dose rates of 10.4, 20.4, 40, 87, 169, 185 and  $280 \mu\text{Gy h}^{-1}$ , respectively.

respectively. By applying different dose rates of the radioisotopes to the buffer solution, the cathodic peak currents were increased, while, the anodic peak currents were decreased. This behavior is related to the formation of  $\text{H}_2\text{O}_2$  due to irradiation of the buffered solution [20]. In fact, the absorption of gamma rays emitted from  $^{201}\text{Tl}$  or  $^{99\text{m}}\text{Tc}$  in a watery medium resulting in ionization and/or excitation, causes free radical formation. In a watery medium, free radicals may act as either oxidizing or reducing agents or can form  $\text{H}_2\text{O}_2$  when they react with water [21]. Accordingly, irradiation of buffered solution by radioisotopes leads to the production of  $\text{H}_2\text{O}_2$ . As illustrated in Scheme 1, based on enzymatic reactions a-c, the produced  $\text{H}_2\text{O}_2$  at AQ-HRP on GC interface increases the peak current.

#### Determination of $^{201}\text{Tl}$ or $^{99\text{m}}\text{Tc}$ Dose Rate

The biosensor response was evaluated for the gamma emitter dose rate determination using amperometric technique. Figure 3 displays amperometric responses of the biosensor

toward the dose rates of  $^{201}\text{Tl}$  or  $^{99\text{m}}\text{Tc}$ , respectively. As can be seen, at a constant voltage of  $-550 \text{ mV}$  (vs. Ag/AgCl), after a transient decay, a steady state current was produced in a reasonable response time of 30 s. The insets in Fig. 3 (A and B) show the calibration curves of the proposed biosensor for the dose rate determination of  $^{201}\text{Tl}$  or  $^{99\text{m}}\text{Tc}$ , respectively. As can be seen, the biosensor responses depend linearly on the concentration of  $\text{H}_2\text{O}_2$  generated due to irradiation of buffered solution.

One of the most probable limitations for HRP enzymatic reaction is suicide inactivation *via* over-production of  $\text{H}_2\text{O}_2$  [22]. However, by comparing the current response produced at highest dose rates (Figs. 3A and B) with the calibration curve illustrated in Fig. 1, one may assume that such a low concentration range of  $\text{H}_2\text{O}_2$  (nM scale) is not high enough to saturate HRP-AQ. In addition, the consistency of redox potentials in Figs. 2A and B with that in Fig. 1 indicates that in the applied dose rate range of gamma ray, the produced  $\text{H}_2\text{O}_2$  did not damage the HRP. This was expected because the

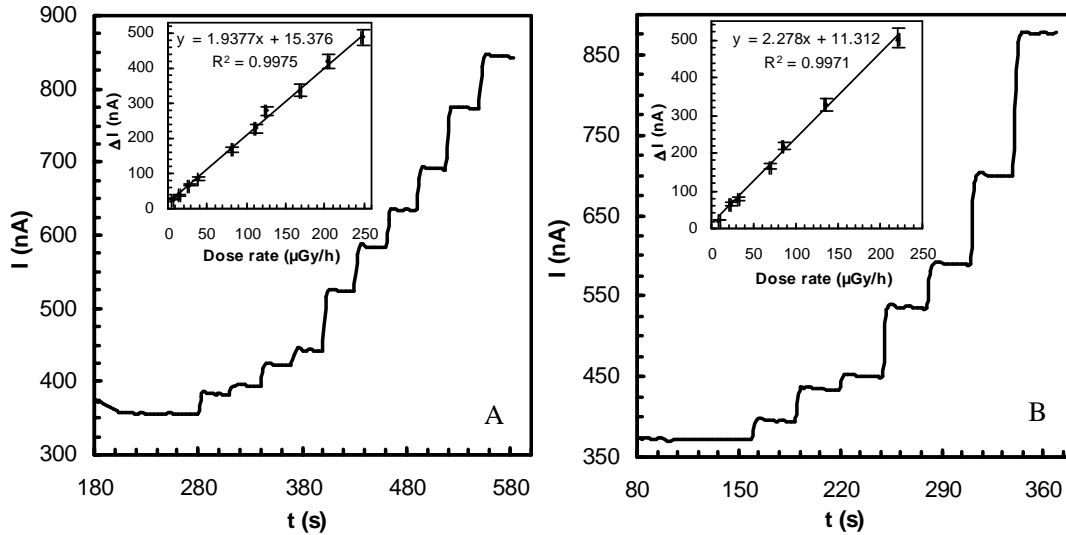


**Fig. 3.** (A) Amperogram obtained by HRP-AQ on GC electrode in the presence of  $^{201}\text{Tl}$ . The steps from down to up was obtained by addition of  $^{201}\text{Tl}$  with dose rates of 0, 6.5, 13.6, 25.9, 38, 81, 111, 125, 169 and 205  $\mu\text{Gy h}^{-1}$ . The inset represents the  $\Delta I$  against  $^{201}\text{Tl}$  dose rate. (B) Amperogram obtained by HRP-AQ on GC electrode in the presence of  $^{99\text{m}}\text{Tc}$ . The steps from down to up was obtained by addition of  $^{99\text{m}}\text{Tc}$  with the dose rate of 0, 9.3, 22.8, 32.9, 69, 85, 135 and 221  $\mu\text{Gy h}^{-1}$ . The inset represents the  $\Delta I$  against  $^{99\text{m}}\text{Tc}$  dose rate. All experiments were done in the PBS at constant potential of -550 mV (vs. Ag/AgCl). Each point represents the average value of three different electrodes.

gamma energies of  $^{201}\text{Tl}$  (75 KeV) and  $^{99\text{m}}\text{Tc}$  (140 KeV) have been categorized as low energy gamma ray emitters.

**Correlation of Gamma Emitter Dose Rate and  $\text{H}_2\text{O}_2$**

To observe the correlation between current response obtained by HRP-AQ on GC electrode toward standard  $\text{H}_2\text{O}_2$  solutions and the  $\text{H}_2\text{O}_2$  produced either by  $^{201}\text{Tl}$  or  $^{99\text{m}}\text{Tc}$ , the regression equation represented in Fig. 1-inset (Eq. 1) was combined with the regression equations obtained by either Fig. 3A-inset (Eq. 2, for  $^{201}\text{Tl}$ ) or Fig. 3 B-inset (Eq. 3, for  $^{99\text{m}}\text{Tc}$ ). Then, based on the obtained Equations of 4 and 5, the plots showing the linear correlation between gamma emitter dose rates and  $\text{H}_2\text{O}_2$  concentrations were established (Fig. 4).

$$\Delta I = 0.353 [\text{H}_2\text{O}_2] + 11.094 \quad (1)$$

$$\Delta I = 1.937 (\text{dose rate of } ^{201}\text{Tl}) + 15.376 \quad (2)$$

$$\Delta I = 2.278 (\text{dose rate of } ^{99\text{m}}\text{Tc}) + 11.312 \quad (3)$$

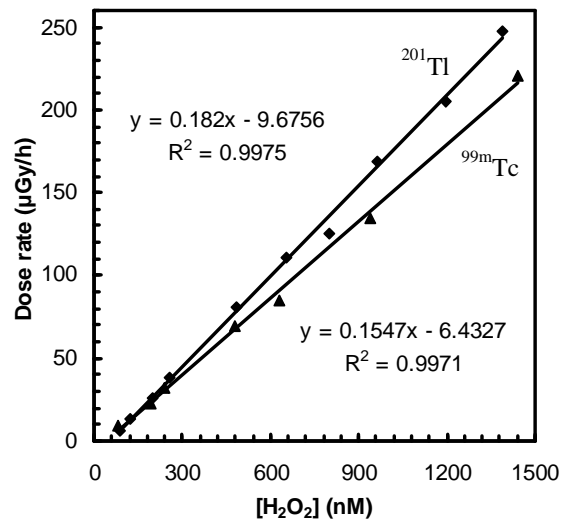


**Fig. 4.** Correlation between the dose rates of  $^{201}\text{Tl}$  (squares) or  $^{99\text{m}}\text{Tc}$  (triangles) and  $\text{H}_2\text{O}_2$  concentration. Each series of points (square or triangle) was calculated based on the Eqs. 2 and 3 respectively.

Dose Rate Determination of Gamma Rays Emitted by Thallium-201

$$\text{Dose rate of } ^{201}\text{Tl} = 0.182 [\text{H}_2\text{O}_2] - 9.6756 \quad (4)$$

$$\text{Dose rate of } ^{99\text{m}}\text{Tc} = 0.1547 [\text{H}_2\text{O}_2] - 6.4327 \quad (5)$$

As shown in Fig. 4, a difference in the slope of regression lines is observed for  $^{201}\text{Tl}$  ( $0.182 \mu\text{Gy h}^{-1}$ ) and  $^{99\text{m}}\text{Tc}$  ( $0.155 \mu\text{Gy h}^{-1}$ ). As seen in the insets of Fig. 3 (A and B), such a difference is also observed in the sensitivity of the proposed biosensor (the slope of calibration curve) for  $^{99\text{m}}\text{Tc}$  ( $2.278 \text{ nA h } \mu\text{Gy}^{-1}$ ) and  $^{201}\text{Tl}$  ( $1.937 \text{ nA h } \mu\text{Gy}^{-1}$ ). These differences may be attributed to the differences in photoelectric effect. (Photoelectric effect is described as an interaction between a gamma ray photon and a bound atomic electron of absorbing environment. As a result, the photon of incident gamma ray is completely absorbed by the atoms and the energy absorbed is used to eject an electron from the atom. Consequently, the photon disappears and one of the atomic electrons, usually from K shell, is ejected as a free electron, called the photoelectron). The gamma energies of  $^{201}\text{Tl}$  and  $^{99\text{m}}\text{Tc}$  are about 75 KeV and 140 KeV, respectively. Therefore, the photoelectron generated by  $^{201}\text{Tl}$  is lower than that produced by  $^{99\text{m}}\text{Tc}$ . Consequently, the generated  $\text{H}_2\text{O}_2$ , due to the interaction between certain dose rates of  $^{99\text{m}}\text{Tc}$  and watery medium is higher than that produced by the same dose rate of  $^{201}\text{Tl}$ .

## CONCLUSIONS

Gamma ray monitoring is of great importance in various fields such as radiology, environmental monitoring, medical treatments and determination of the absorbed dose in the body exposed. It seems that, due to characteristics such as simplicity, high sensitivity, low detection limit, and negative redox potential, the HRP-AQ-based biosensor would have potency to be used as a novel commercial detector for a reliable monitoring of gamma ray emitted from  $^{201}\text{Tl}$  and  $^{99\text{m}}\text{Tc}$  in aqueous samples. Further investigation in this respect is being currently pursued by our team.

## ACKNOWLEDGMENTS

Financial support provided by the Research Council of the University of Tehran and Baghiyatollah University of Medical

Sciences is gratefully appreciated.

## REFERENCES

- [1] N. Tsoulfanidis, Measurement and Detection of Radiation, 2<sup>nd</sup> ed., Taylor & Francis, Washington, 2005, Chap. 4.
- [2] J.D. Anik, I. Janik, D.M. Bartels, J. Phys. Chem. A 111 (2007) 7777.
- [3] G.R. Sunaryo, Y. Katsumura, I. Shirai, D. Hiroishi, K. Ishigure, Radiat Phys. Chem. 44 (1994) 273.
- [4] M. Mognato, C. Girardi, S. Fabris, L. Celotti, Mutat. Res.-Fund. Mol. M 663 (2009) 32.
- [5] W. Sudprasert, P. Navasumrit, M. Ruchirawat, Int. J. Hyg. Envir. Heal. 209 (2006) 503.
- [6] M. Fattahi, C. Houée-Levin, C. Ferradini, P. Jacquier, Int. J. Rad. Appl. Instrum. 40 (1992) 167.
- [7] A.C. Pappas, C.D. Stalikas, Y.C. Fiamegos, M.I. Karayannis, Anal. Chim. Acta 455 (2002) 305.
- [8] H. Hwang, P.K. Dasgupta, Anal. Chim. Acta 170 (1985) 347.
- [9] B.V. Chikkaveeraiah, H. Liu, V. Mani, F. Papadimitrakopoulos, J.F.A. Rusling, Electrochem. Commun. 11 (2009) 819.
- [10] S. Lu, J. Song, L. Campbell-Palmer, Sciatica Horticulture 120 (2009) 336.
- [11] B.Z. Zhu, H.T. Zhao, B. Kalyanaraman, B. Frei, Free Radical Bio. Med. 32 (2002) 465.
- [12] Z.S. Wu, S.B. Zhang, M.M. Guo, C.R. Chen, G.L. Shen, R.Q. Yu, Anal. Chim. Acta 584 (2007) 122.
- [13] N. Mogharrab, H. Ghourchian, Electrochem. Commun. 7 (2005) 466.
- [14] N. Mogharrab, H. Ghourchian, M. Amininasab, Biophys. J. 92 (2007) 1192.
- [15] M. Bradford, Anal. Biochem. 72 (1976) 248.
- [16] S. Kang, S. Kwok-Keung, J. Electroanal. Chem. 574 (2004) 63.
- [17] M. Shourian, H. Ghourchian, Sens. Actuators B 145 (2010) 607.
- [18] T. Ruzgas, E. Csöregi, J. Emnéus, L. Gorton, G. Marko-Varga, Anal. Chim. Acta 330 (1996) 123.
- [19] R. Maidan, A. Heller, Anal. Chem. 64 (1992) 2889.
- [20] M. Bickel, L. Holmes, C. Janzon, G. Koulouris, R.

Shourian *et al.*

- Pilvio, B. Slowikowski, C. Hill, Appl. Radiat. Isot. 53 (2000) 5.
- [21 ] T.H. Zastawny, M. Kruszezowski, R. Olinski, Free Radical Bio. Med. 24 (1998) 1250.
- [22 ] P.N. Bartlett, P. Tebbutt, R.G. Whitaker, Prog. React. Kinet. 16 (1991) 55.